ASEAN Engineering Journal

Full Paper

POWER LOSS MITIGATION IN A DISTRIBUTED PHOTOVOLTAIC-BASED MICROGRID USING SMA-PSO DUAL-OPTIMIZATION TECHNIQUE

Mallam Terab Ali, Syed Norazizul Syed Nasir*

Faculty of Electrical Engineering, Universiti Teknologi Malaysia, 81310, UTM Johor Bahru, Johor, Malaysia

Article history
Received
3 September 2024
Received in revised form
02 December 2024
Accepted
08 July 2025
Published online
28 February 2026

*Corresponding author
syednorazizul@fke.utm.my

Graphical abstract

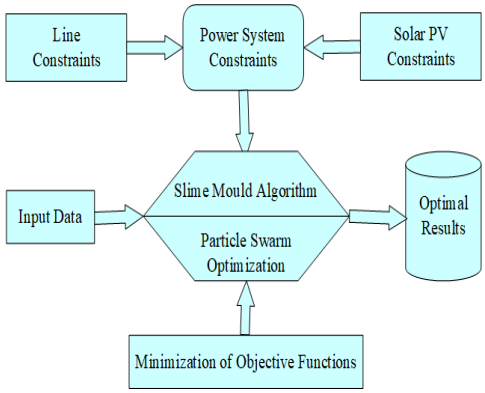

Abstract

The renewed research interest in renewable energy generation has substantially reduced the cost of electricity production from these sources and has laid the strong foundation for competing with non-renewable sources. The optimum power flow (OPF) problem involves addressing the unpredictable limitation by determining appropriate values for the control variables and optimizing the objective functions. The main constraint faced in the conception and design of power systems is the propensity for voltage instability. This paper proposed a Slime mould algorithm (SMA) and Particle swarm optimization (PSO) in an SMA-PSO dual-optimization that dynamically adjusts the number of search agents in the same search space using the SMA's feedback capacity and the PSO's quick convergence mechanism. The suggested algorithms were tested on the IEEE 33 bus system. The result indicates a decrease in network real power loss of 49.64% with a significant redundancy stabilization power of 910.9771 kW. This substantial decrease is sufficient to stabilize the microgrid while integrating a 3,500 kW Photovoltaic (PV) generator at the optimal location bus 6. The SMA-PSO technique validates further efficacy when compared to previously published research works on either single or hybrid optimisation approaches. Future research may include adding more complex microgrids with more buses and exploring duality and hybridization optimisation techniques

Keywords: Slime Mould Algorithm; Particle Swarm Optimization; Dual-Optimization; Power Loss; PV-Integration.

1.0 INTRODUCTION

The foremost goal of electrical power optimization in an optimal power flow (OPF) problem is to minimize the cost of power generation to reduce the capital expenses on plant conception. Consequently, the system constraints should be kept within tolerable ranges to sustain acceptable voltage magnitude, line flow conditions and system stability [1]. Extensive research in renewable energy generation has significantly decreased the cost of power produced from these sources and has established a foundation for competing with non-renewable sources [2, 3]. Projections indicate that, despite the many benefits of renewable energy compared to fossil fuels, the dominance of fossil fuels over renewable energy will increase in the next twenty years [4, 5]. Nevertheless, in situations where there is a heavy load and a line outage contingency, relying solely on the voltage limit constraint may not be enough to maintain a stable voltage level [6]. Instead, the main focus of the objective function should be on enhancing voltage stability to ensure the reliability of the system [7, 8]. The major goal of electric utility organizations is to constantly look for economically operational situations and optimum power generation schedules to minimize the cost of power generation while meeting reliability constraints and power transfer limitations [9].

The OPF is a complex system that requires finding the feasible values for the control variables of a system in order to optimize the objective function. This must be done while taking into account different equality and inequality constraints [9 1]. Interestingly, by taking a peculiar review of the prevailing consequences of voltage collapse scenarios, several OPF

techniques have been developed and successfully used for various objectives relating to the electrical power system [10]. The OPF considered one of the most viable techniques for efficient planning and controlling the operation of power systems [11].

The primary limitation encountered in the development and design of power systems is the propensity for voltage instability [12]. Reactive power may be introduced in certain areas where it is difficult to maintain voltage stability and limits. By using this technique, the voltage profile and stability may be maintained with the assistance of an induction generator [13, 14]. Furthermore, in most OPF-related problems, objective functions are usually assigned to reduce the cost of fuel consumption or line losses [15]. The load flow analysis (LFA) should be run initially to determine appropriate bus voltages and line parameters. However, voltage instability and voltage collapse index can also be considered in some rear scenarios [16]. When employing various combinations of control variables for power settings, it is crucial to consider the power balance between generation and load consumption [17]. However, the solution of the power flow equation needs to be revised for the appropriate operation of the power system since only a few powers system setting combinations can accomplish the economical and reliable operation of the complete power system network [18].

Several factors, including system efficiency, environmental advantages, and transmission congestion management, have led to the emergence of a new field in the electric power system [19]. The primary component of this new study subcomponents in power system is the deployment of many distributed generation (DG) units near load centres, rather than extending the capacity of a single generating station [20]. DG may originate from several sources and technologies. Electricity generated from renewable sources such as wind, sun, and biomass are often referred to as 'renewable energy' [21].

Similarly, there has been a growing interest in integrating goals from other categories in order to develop optimal solutions that simultaneously satisfies both economic and technological criteria. As optimization challenges continue to evolve, several strategies have been created to provide a solution for the OPF challenges [22]. Various authors have addressed the answer to the OPF issue, using both traditional and modern optimization strategies. Metaheuristic optimisation methods are often used in many technical and industrial applications to solve single- and multi-objective optimisation problems, with the goal of optimizing one or more objective functions. The algorithms outlined in the literature can be classified into three main categories based on some defining characteristics: Evolutionary physics-based, Swarm Intelligence and Traditional optimization techniques [23].

Recently, some authors conceived and implemented various metaheuristics algorithms to tackle the challenges of the OPF problems. These optimizations methods can be broadly grouped into classical, conventional, and modern optimizations algorithms. Compared to the latter, the former converges faster into the global optima. Modern optimisation algorithms may be categorized into three classes: metaheuristic optimisation algorithms (MAs), artificial intelligence-based optimisation algorithms (AI), and a mix of the two approaches. Modern optimisation techniques have been developed and validated in power system analysis to efficiently discover the best solution for the OPF issue in power systems of various sizes [24].

Nowadays, the AI approach and metaheuristic-based optimization techniques have been mainly adopted to complement distribution networks to meet consumer load demand [24 9]. This method has the benefit of being able to tackle a wide range of optimization issues by focusing just on inputs and outputs. Several metaheuristic methods, such as Genetic Algorithm (GA), Evolution Programming (EP), Ant Colony Search Algorithm (ACSA), Tabu Search (TS), Simulated Annealing (SA), Harmony Search Algorithm, Artificial Bee Colony (ABC), Bacterial Foraging Optimizations Algorithm (BFOA), Firefly Algorithm (FA), Cuckoo Search Algorithm (CSA) and Runner Root Algorithm (RRA) and Particle Swarm Optimization (PSO), have been proposed in many literatures to achieve the tolerable minimum threshold in power losses [25-27]. Haris Hawk Optimization (HHO) was introduced by [28] which reduces system losses by 9.84%. Interestingly, nowadays, the Slime Mould Algorithm (SMA) optimizations approach has gained tremendous attention in recent literature [28 7]. Specifically, the hybridization, duality and combination of two or more optimization tools have been more efficient techniques for solving system reconfiguration problems [29, 30].

The authors in [31] proposed hybridization of SMA and PSO to non-symmetrical theoretical problems. The study was not adopted for practical applicability. In a hybrid optimization technique, the study in [32] proposed a GWO-FPA to solve optimization problems with or without unknown search areas. In a similar approach, the authors in [33] presented PSO-GSA for efficient energy spectrum sensing in cognitive network. In a new hybrid optimization approach the authors in [34] presented PSO-GWO. However, the proposed algorithm was testing on parameter estimation, flow sheeting and leather nesting problems. The researchers in [35] proposed a PSO-GWO to optimize a microgrid in terms of least cost option and the study covered up to 93% of the load demand.

The main goal of dual-optimization technique is to discover the best scheduling of specific control variables and leverage on strength and improve on weaknesses of one tool against the other while keeping the system restrictions within their allowable boundaries [35, 36]. Irrespective of the many approaches, the shared attributes that are present are the traits of exploration and exploitation. In the exploitation stage, the algorithm aims to discover a globally optimum solution by focusing on strengthening the search process inside a specific small area rather than the whole search space [36, 27]. However, these algorithms' performances can be improved, especially the computational time and other faster convergence properties [37, 10].

To search for nourishment, the slime mould mimics oscillating feedback attitude. SMA is known for efficient global search capacity and its more recent proposal to address single-objective optimization issues in are its most notable features. Many engineering design issues and applications have previously used the SMA. Several areas have successfully used SMA to tackle multi- objective optimization problems, according to a quick survey of the related literature.

This research reports that SMA's capacity to mimic slime's bio- inspired behaviour, including its foraging attitude and morphological alterations, is the key differentiator between SMA and other metaheuristic algorithms [38, 9]. Nevertheless, its whole life cycle simulation is not considered. SMA weight simulates the two-way feedback that slime mould produces during foraging. Similarly, if there's a lot of food in one place, it's

quite unlikely that slime will leave that region. The primary benefit of SMA is its capacity to be adopted into complex environments and its expanded computing capabilities [39 1]. The decentralized nature of this technique enables parallelism, making it well-suited for multitasking processes [40, 7]. The drawbacks of SMA include its susceptibility to parameter selection, impact from external environmental variables, and inherent lack of scalability in large-scale data applications.

The particle swarm optimization (PSO) is a bio-inspired evolutionary stochastic algorithm that was initially conceived by James Kennedy and Russel Eberhart in 1995 [40, 16]. The effectiveness of this algorithm, which draws inspiration from the social behaviour of creatures like bird flocking and school of fish, has been shown in the optimization of Multi-objective problems. The PSO is an algorithm that uses a population-based search method. In this algorithm, people, referred to as particles, dynamically alter their locations (states or positions) over a given period [40, 36]. Within a PSO system, particles navigate across a search space that encompasses many dimensions. The benefits of PSO are its simplicity of implementation and the limited number of parameters that need to be adjusted [40].

The relatively famous SMA-PSO duality are adopted because of their robustness in application to engineering design problems, simplicity in applications to optimal multi-constraints situations and high precision capabilities in solving rather complex multi objective scenarios [41-43]. This study examines the optimal placement of a solar photovoltaic (PV) generator in a microgrid and tested on the popular IEEE 33-bus system. The proposed technique leverage on the feedback mechanism of SMA and fast convergence capability of PSO which was subjected to the same convergence parameters. This approach basically used to optimise the network reliability by mitigating real power losses in a hybrid radial microgrid. The validity of the proposed algorithms is shown by its application to the optimal location and integration of photovoltaic distributed generation. This can be achieved by determining the most efficient configurations of the generator terminal voltages, optimal bus location and minimizes power losses [43, 12].

The key contributions of this paper can be summarized as follows;

i. The modified SMA-PSO are used to solve multi-objectives OPF challenges by subjecting the iteration process to the same convergence parameters in a dual optimization approach.
ii. The SMA-PSO approach utilizes the feedback capacity of the SMA and incorporates the fast convergence mechanism of the PSO to dynamically adjust the number of search agents within the search space.
iii. The integration of modelled PV to the IEEE 33 bus system to enhance the system reliability index

2.0 METHODOLOGY

Low voltage and high characteristics in radial distribution microgrid system leads to increase in power losses comparatively [44, 39]. Few research studies were reported on finding optimal location of DGs and sizing under variable loading conditions. However, in this paper, the following procedures were adopted to implement the proposed SMA-PSO approach.

2.1 Slime Mould Algorithm

2.1.1 Methods of Food Approaching

The proposed model simulates the coiling behaviour of slime mould and its approach to foraging as described by equation (1), (2) and (3).

$$\overrightarrow{X_t} = \begin{cases} \overrightarrow{X_{b(t)}} + \overrightarrow{v_b}\left(\overrightarrow{W}.\overrightarrow{X_{a(t)}} - \overrightarrow{X_{b(t)}}\right), r < p \\ \overrightarrow{v_c}X_{b(t)}, r \geq p \end{cases} \quad (1)$$

$\overrightarrow{v_c}$ is a parameter that decreases linearly from one to zero, *t* denotes the number of iterations, v_b is a given parameter within the range of -*a* to *a* defined by equation (2) while $\vec{x}$ represents the individual location with the greatest odour, $\overrightarrow{X_t}$ denotes the position of slime mould at the iteration *(t)* and $\vec{x}a, \vec{x}b$ two individuals chosen randomly from the swarm *w*, $\overrightarrow{W}$ indicates the weight of slime mould as *P* represents the size of the population defined in equation (3) while *r* is random values between 0 and 1.

$$a = \operatorname{arctanh}\left(-\left(\frac{t}{t_{\max}}\right) + 1\right) \quad (2)$$

$$P = tanh|S(i) - DF| \quad (3)$$

Let *i* represent the fitness of *(X)* and DF denote the greatest fitness attained in all iterations. When the scenario reaches a state denoted as S(i) and represents the first half of the population, the variable r is assigned randomly picked values from the interval [0, 1] at regular intervals.

2.1.2 Food wrapping

Equation (4) below is the mathematical algorithm for updating the location of slime mould:

$$\overrightarrow{W}(smellindex) = \begin{cases} 1 + r \cdot log\left(\frac{bF - S(i)}{bF - wF} + 1\right), condition \\ 1 - r \cdot log\left(\frac{bF - S(i)}{bF - wF} + 1\right), \ others \end{cases} \quad (4)$$

When S(i) reaches the first half of the whole population, r represents a random number between 0 and 1, and bF is equal to the optimum fitness obtained in the current iteration phase. The variable wF represents the lowest level of fitness attained during the current iteration phase. The SmellIndex value represents the ordered series of fitness values in a minimal value issue, sorted in ascending order [44, 1]. Equation (5) shows the food wrapping behavior of slime mould.

$$\overrightarrow{X^*} = \begin{cases} rand.(UB - LB) + LB, rand < z \\ \overrightarrow{X_{a(t)}} + \overrightarrow{v_b}\left(\overrightarrow{W}.\overrightarrow{X_{a(t)}} - \overrightarrow{X_{b(t)}}\right), r < p \\ \overrightarrow{v_c}\overrightarrow{X_{(t)}}, r \geq p \end{cases} \quad (5)$$

LB and *UB* denotes the minimum and maximum boundaries of the search intervals, whereas *rand* and *r* symbolise random values that fall within the range of 0 to 1. The variable z is a range that extends from 0 to 0.1. The remaining parameters are as defined in equation (1). Figure 1 shows the modified flow chart of the SMA algorithm

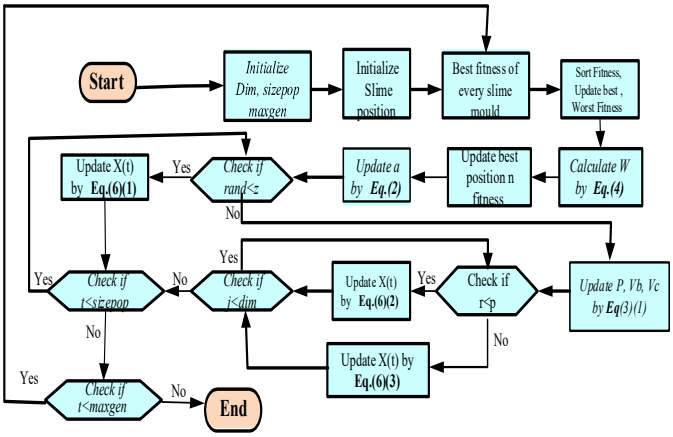

Figure 1 Modified Slime Mould Algorithm Flow Chart [44, 40]

2.2 Particle Swarm Optimization

The PSO algorithm simulates the general collective behaviour of a swarm of insects [45, 12]. Every individual or particle exhibits dispersed behaviour by using its intellect and being impacted by the collective behaviour of the group [46, 29]. This approach enhances issue optimization by manipulating people within the problem's domain using the optimum function for the swarm's location *(Xz)* and velocity *(Vz).* During each iteration, every person in the population will update their position based on two key values: the optimum solution for that respective individual *(pbest*) and the optimum solution found in the entire population swarm (*gbest).* Figure 2 described a modified flow chart of PSO algorithm.

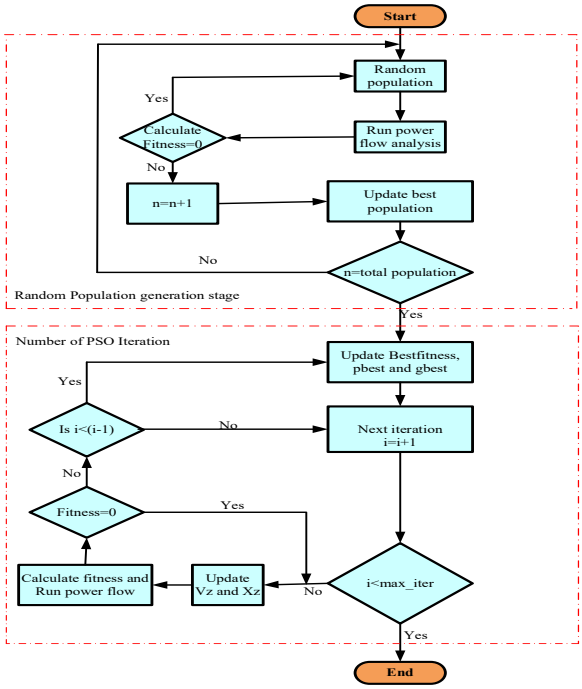

Figure 2 Flow Chart of PSO modified from [46, 29]

Furthermore, once the two optimal values have been acquired, the location and velocity of each member of the swarm movement will be updated by equations (1) and (5). Where *Xz(i)* represents the number of individual particles in the population at position X, and *Vz(i)* is the velocity vector of each particle in the population while *gbest* and *pbest* are the global best solution of the whole population and best solution of individual particles in the population respectively.

The PSO algorithm initiates by creating a random population size of particles. It involves using the Individual assessment and power flow functions to choose particles with optimal fitness values. The two values of pbest and gbest results will dictate modifications to the speed value throughout the process of updating individual variables [46, 13]. The previous individual's value will be reassessed using individual validation function and power violation functions to obtain the optimum updated values of the pbest as well as gbest. The operation will proceed until the pegged iterations number is reached.

2.3 The IEEE 33 Bus System

The IEEE 33-bus radial distribution test feeder serves as a standard system for evaluating techniques, approaches, and solutions pertaining to power distribution systems in research and engineering projects [46 42]. It comprises of a range of distribution systems with different sizes and features, designed specifically for benchmarking, research simulations in laboratories and network optimization [46 22].

i. Network topology: The system has 33 buses arranged in a radial topology, where electricity is transmitted from a single source (substation) over distribution lines to loads (consumers) [46 2].

ii. Model Loading: The feeder incorporates a diverse range of loads, including residential, commercial, and industrial loads, each having distinct features and demand patterns [47 30].

iii. The branch parameters include the characteristics of the distribution lines and equipment, including line impedances, lengths, and topologies. These parameters are designed to replicate the properties of actual distribution network [47 44].

iv. Voltage regulation is achieved by including voltage regulators and capacitors into the system, which helps to ensure that voltage levels remain within acceptable limits throughout the network [48 45].

The IEEE 33-bus radial distribution system is used by researchers for applications, including as

a. Testing and evaluating algorithms related to the optimum functioning, reconfiguration [48 46].

b. Evaluating the effects of dispersed generation, the integration of RE and DSM.

c. Investigating the efficacy of protection and coordination strategies in detecting faults.

Figure 3 indicates the single line diagram of IEEE 33 bus system and optimal bus location of PV integration.

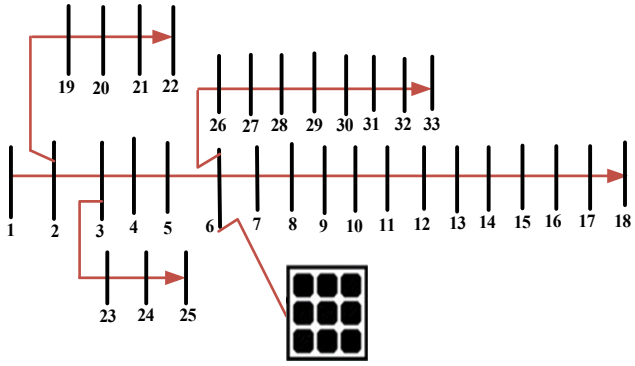

Figure 3 IEEE 33-bus sytem with optimal PV location modified from [7]

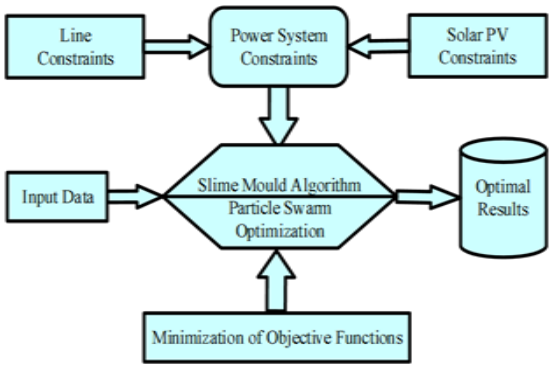

Figure 4 SMA-PSO dual optimization technique modified from [7]

The red lines in figure 3 represents the direction of power flow and the black vertical lines shows distribution bus feeders. The IEEE 33-bus radial distribution system is used to compare various methods for addressing difficulties and enhancing the operation and planning of power distribution systems.

2.4 Problem formulation

2.4.1 Objective Functions And Constraints

The objective function of the proposed study is the optimal DG location and minimize overall system loss. The power flow formulas to analysis the real and reactive powers are when the PV is integrated is given by equations 6 and 7.

$$\mathrm{P}_{i-1} = \mathrm{Pi} + P_{L,i} + \mathrm{R}_{i-1,i}\left(\frac{P+jQ}{|V|}\right) - \mathrm{P}_{DG,i} \quad (6)$$

$$\mathrm{Q}_{i-1} = Qi + Q_{L,i} + x_{i-1,i}\left(\frac{P+jQ}{|V|}\right) - \mathrm{Q}_{DG,ui} \quad (7)$$

Where *Pi* and Qi are active reactive powers transmitted through the line buses *i* while $P_{L,i}$ and $Q_{L,i}$ are active and reactive power losses at the buses *i* and $R_{i-1,i}$ and $X_{i-1,i}$ are the resistance and reactance of the branch feeder. $\mathrm{P}_{DG,i}$ and $\mathrm{Q}_{DG,ui}$ are the real and reactive powers injected by DG at bus *i.* Therefore, the power loss, both active and reactive, between bus i and i+1 may be calculated using equations (8) and (10). The network is assumed to be balanced and associated with each bus are four inevitable quantities: active power Pi, reactive power Qi, voltage magnitude V, and voltage angle θ.

$$P_{loss} = Ri_{(i+1)} * Ii^2 \quad (8)$$

To minimize the losses the objective function is given by

$$min\mathrm{F}(obj) = \sum_{i=1}^{N} \mathrm{w1} * (Ploss) + \sum_{i=1}^{N} \mathrm{w2} * (Vi - 1)^2 \quad (9)$$

W_1 and W_2 are weighting factors with priority to power loss and voltage deviation respectively while *Vi* represent the bus voltage

$$P_{loss}\,,\ T = \sum_{i=1}^{N}(Ploss, i) \quad (10)$$

Figure 4 shows the formulation of dual optimization technique of SMA and PSO algorithms with constraint and input data.

2.5 System/Problem Constraints

The node equation can be used to depict how network bus voltages and currents relate to one another [49, 14]. Further integration of PV will lead to power surges at certain buses, therefore, the need to enforce some equality and inequality constraints to limit the voltage levels [50]. Equations (11) and (12) represent the model's equality and inequality requirements.

$$V_{min} \le Vi \le V_{max} \quad (11)$$

$$P_{min} \le P_{inj} \le * \ 0.4 \quad (12)$$

Where *Vmin* and Vmax are the maximum voltage limits at ith bus and *Pmin* and *Pinj* are the minimum and maximum power of the injected DG at the optimal bus. *Pinj* is fixed at 0.4* to limit the maximum power to be injected not to exceed 40% of the total power requirement [51].

i. Power Balance Condition

Another important constraint formulated is the power balance between generation and demand or consumption. Thus, the limits must be as defined in equation 13.

$$\sum_{h=1}^{24} P_{slack} + P_{pv} - P_{loss} - P_{demand} \quad (13)$$

Where *Pslack* is the generated power, *Ppv* the integrated photovoltaic, Ploss is the system power losses and *Pdemand* the power demand for consumption during the 24 hours of consideration.

ii. PV size integrated as DG

The next constraint is the size of the solar photovoltaic integrated generation [51 14 4]. Equation 14 depicts the ranges of the DG size. Though already pegged at less than or equal to 40% of the base generation, the model of the DG should be within the minimum and maximum values of the following.

$$\sum_{24} P\left(\frac{min}{pv}\right) \le P_{pv} \le \sum_{24} P\left(\frac{min}{pv}\right) \quad (14)$$

Input parameters before running the power flow analysis includes bus data, bus type, initial voltage, active and reactive demands voltage limits generator data and line data. After running the power flow output parameters are voltage profile, active and reactive powers, generation levels, fitness values, local global best solutions as well as updated positions and voltages.

iii. Iteration procedure

The iteration procedure for the dual optimization approach was carried out based on the following descriptive steps

Step 1: Run the power analysis to determine the suitable bus voltages and line current parameters of the microgrid [53 54].

Step 2: Define the same input parameters of both SMA and PSO.

a. Objective functions, decision variables and basic convergence parameters.
b. Population size of search agents.
c. Maximum iteration and optimization boundaries with same step size increase.
d. System equality and inequality constraints and tolerance limits.
e. Set a penalty parameter for violating a constraint.
f. Addition of scaling functions to normalize the algorithms.
g. Set stopping criteria to either maximum iterations, convergence or tolerance violations.

Step 3: The integration of the DG is implemented at a stepwise increase of 500 kW (starting from 2000kW to 4000 kW) until a saturation power is obtained. The saturation peak power is the point at which any further increase in integration power will not affect the already obtained values significantly.

Step 4: On reaching any of the stopping criterion, the best values of the objective functions are evaluated and recorded. Then a subsequent increase in the integration power is considered and repeatedly the corresponding values of interest are recorded.

Step 5: When all the set conditions were achieved for optimum DG location bus, power losses and iteration convergence of the two algorithms, the average values are recorded as SMA-PSO new parameters. Figure 5 shows the power and voltage parameters before integration of DG.

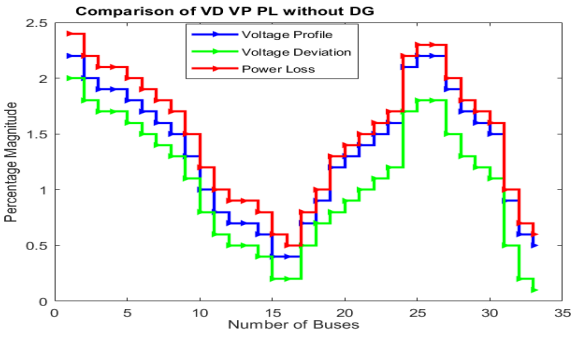

Figure 5 Comparison of power and voltage parameters without DG

3.0 RESULTS AND DISCUSSION

The evaluation of the optimal bus size and location for PV integration was conducted on the widely used 33-bus radial distribution network, as seen in Figure 3. The aggregate apparent load of the system is 4.3694 MVA. This research examines the incorporation of PV as DG to enhance active power generation while minimizing system losses and achieving optimum integration at the bus level.

3.1 Initialization

The design was derived from the execution of the SMA and PSO concurrently, which forecasts the optimal positioning of solar photovoltaic (PV) systems as distributed generation (DG). The forward and backward LFA to establish the appropriate line parameters of the design on the IEEE 33 bus. All the simulation programs and the codes were run on a Processor Intel(R) Core i5-6300U CPU @ 2.40GHz Latitude E5570 Dell Laptop with Microsoft Windows 10 MATLAB R2023b software package. The Mvar of the generator buses was evaluated at all the iterations. The Vm(n) is increased in increments of 0.01 per unit (pu) in order to bring the generator Mvar within the specified limits. The system loss prior to the integration of the DG was 202.6771 kW.

3.2 Simulation results

The following results shows the simulation outcome for the various PV integration at the buses to determine the optimal location and the corresponding power losses. In table 1, the application of the SMA results shows saturated microgrid with no excess power for stabilization at the integration of 2000 kW and 2500 kW as all the injected power were directly absorbed by the network. However, the optimum value was to integrate 3500 kW as this gives 26.18% excess power and 49.64% real power losses. Although the penetration of 4000 kW gives up to 38.56% excess power, it recorded a relatively lower real power loss of 49.55%. The optimum location is bus 6, as shown in figure 3 earlier.

Table 1 SMA simulation results

	SMA					
SN	**PV as DG (kW)**		**Selected Bus**		**Power Loss**	**%Loss**
	Initial	**Used**	**Initial**	**Optimal**	**(kW)**	
1	4000	2457.45	31	6	101.90	49.55
2	3500	2583.67	16	6	101.72	49.64
3	3000	2531.46	21	6	101.74	49.63
4	2500	2500.00	24	6	101.79	49.62
5	2000	2000.00	2	7	105.60	49.72

In addition, according to the PSO simulation results in table 2, the microgrid is saturated and does not have any excess power for stabilization when the penetration reaches 2000 kW and 2500 kW, since all the available power is being used by the microgrid. Nevertheless, the most favorable power for integration was determined to be 3500 kW, resulting in a power redundancy of 25.87% and actual power losses of 49.64%. Afterwards, the 4000 kW penetration results in a surplus power of up to 32% and a real power loss of 49.50%. However, this outcome cannot be regarded optimal owing to the expensive nature of higher generating PV plants and the comparatively lesser corresponding decrease in system power losses.

Table 2 PSO simulation results

	PSO					
SN	**PV as DG (kW)**		**Selected Bus**		**Power Loss**	**%Loss**
	Initial	**Used**	**Initial**	**Optimal**	**(kW)**	
1	4000	2720.00	2	6	102.02	49.50
2	3500	2594.38	2	6	101.73	49.64
3	3000	2655.00	2	6	101.81	49.60
4	2500	2500.00	12	6	101.79	49.61
5	2000	2000.00	2	7	105.60	49.72

The following figures illustrate the simulation graphical outcomes for both the SMA and PSO algorithms. The power losses reduction and convergence iterations were seen for all the distributed generation (DG) integrations ranging from 2000 kW to 4000 kW, with an incremental step of 500 kW, as shown in figures 6 to 14.

Figure 6 indicates the average system power losses and voltage parameters with PV as DG integration.

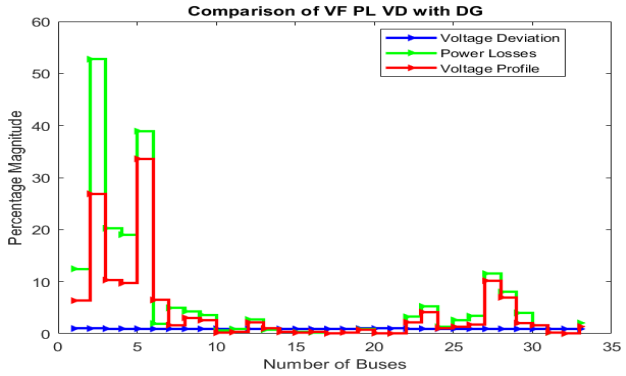

Figure 6 Comparison of power and voltage parameters with DG

The subsequent figures illustrate the convergence of SMA and PSO at various DG sizes and the corresponding system power losses. Figure 7 show SMA convergence at 2500 kW penetration. the system converges immediately within the first 3-iterations. This was also due to the network saturation which absorbs all the power injected. The optimal bus is still bus 6. Though SMA was initially integrated at bus 24 and PSO on bus 12. The power losses were also 101.7924 kW for both algorithms.

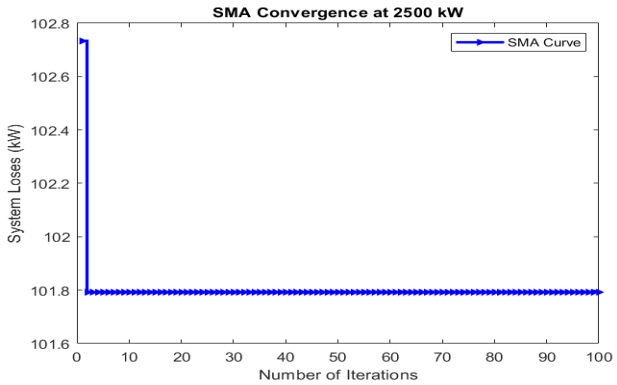

Figure 7 SMA Convergence curve for 2500 kW DG

Figure 8 shows the PSO convergence curve for injected power of 2500 kW magnitude.

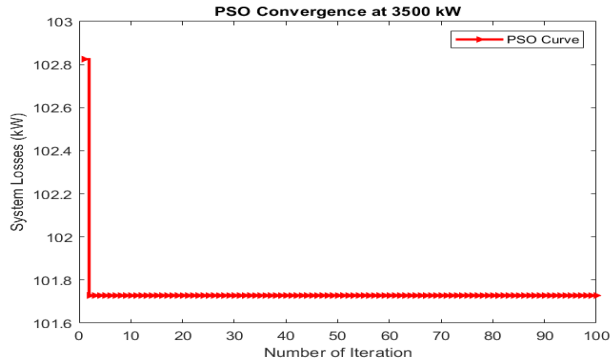

Figure 8 PSO Convergence curve for 2500 kW DG

Figures 9 and 10 depict SMA and PSO convergence at 3000 kW integration. The SMA converges at the 30th iteration in 123.49 secs and power loss reduction of 49.63%, while PSO convergences at 60th iteration in 101.81 secs with 49.59% power losses. The network is stable with 84% and 88% of the injected power utilized to meet the load demand in both algorithms respectively.

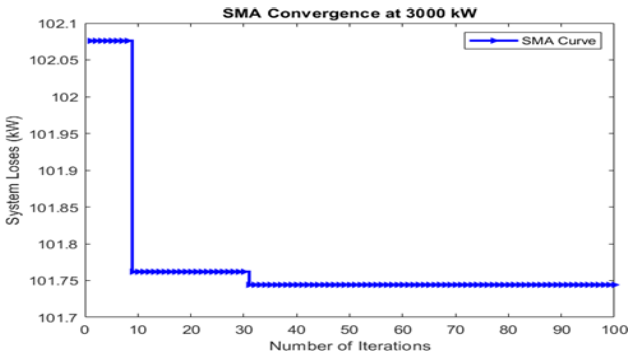

Figure 9 SMA Convergence curve for 3000 kW DG

Figure 10 shows the PSO convergence curve for 3000 kW DG integration power.

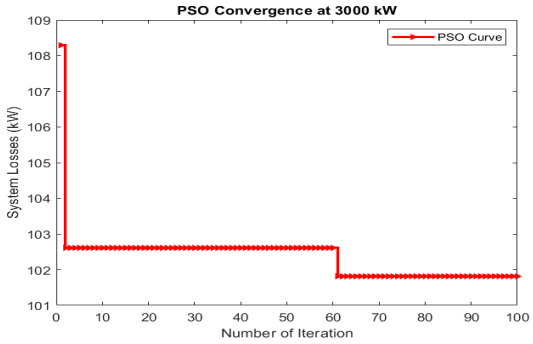

Figure 10 PSO Convergence curve for 3000 kW DG

In a similar scenario the integration of 3500 kW DG reduces the system power losses to 101.7233 kW by SMA and to 101.7281 kW by PSO representing 49.64% respectively as shown Figures 11 and 12, The SMA converges at the 3rd iteration in 125.07 secs while PSO convergences at 2nd iteration in 119.94 secs.

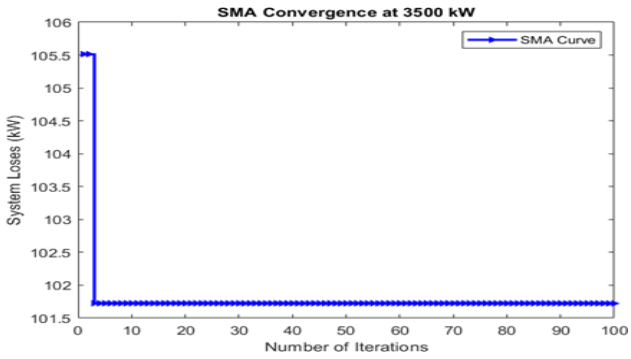

Figure 11 SMA Convergence curve for 3500 kW DG

The network is more stable and reliable with almost 74% of the injected power absorbed to meet the demand in both algorithms respectively. The power redundancy of 26% has further placed the microgrid in more reliable condition in the event of sudden surge in power consumption. The optimal bus is confirmed by both algorithms, which is bus 6. Figure 12 shows the PSO integration of 3500 kW DG power.

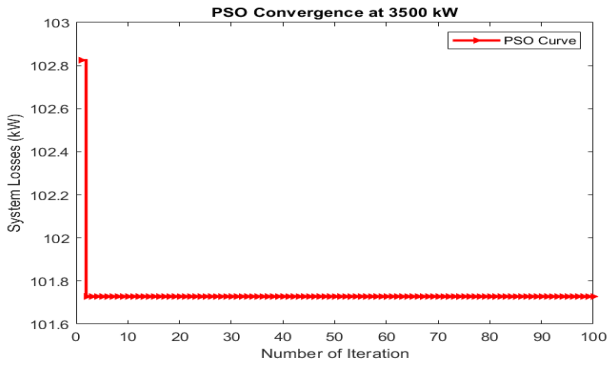

Figure 12 PSO Convergence curve for 3500 kW DG

In figures 13 and 14, when 4000 kW of DG is integrated into the system, the power losses are reduced to 101.9005 kW by the SMA and to 102.0152 kW by the PSO algorithms. This reduction represents 49.55% and 49.50% respectively. The network's excess power of 38% and 32% has significantly improved its stability. Nevertheless, the exorbitant expenses of a larger photovoltaic (PV) plant might place this situation at a significant disadvantage.

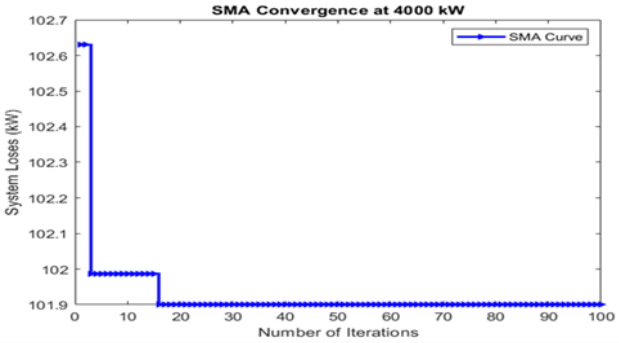

Figure 13 SMA Convergence curve for 4000 kW DG

Figure 14 indicates the PSO algorithm convergence for 4000 kW DG integration.

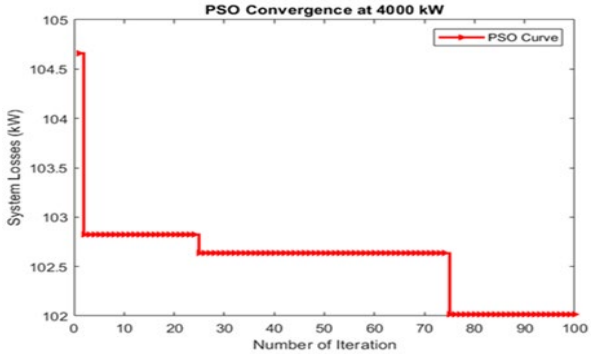

Figure 14 PSO Convergence curve at 4000 kW DG

The SMA reaches convergence after 15th iterations, in 121.30 seconds. On the other hand, the PSO convergence after 75th iterations, in 93.64 secs as shown in figures 13 and 14. The microgrid demonstrates increased stability, with almost 62% and 68% of the injected power effectively used to meet the load requirement in the SMA and PSO algorithms, respectively.

Table 3 presents the average results of the SMA-PSO dual optimisation, which demonstrates that the microgrid reached saturation and achieved stabilisation without any excess power while injecting 2000 kW and 2500 kW. All the produced power was completely absorbed by the microgrid. However, the most favourable option is to integrate 3500 kW, as it represents an excess power of 26.03% and a loss of real power of 49.64%. Even though, the penetration of 4000 kW results in an excess power of up to 38% and a recorded actual power loss of 49.53%, it nevertheless achieved comparatively reduced power losses.

Table 3 SMA-PSO Dual optimization average simulation results

SMA-PSO						
SN	**PV as DG (kW)**		**Selected Bus**		**Power Loss**	**%Loss**
	Initial	**Used**	**Initial**	**Optimal**	**(kW)**	
1	4000	2588.00	31	6	102.96	49.53
2	3500	2589.02	16	6	101.73	49.64
3	3000	2693.23	21	6	101.78	49.61
4	2500	2500.00	24	6	101.79	49.61
5	2000	2000.00	2	7	105.60	49.72

The proposed SMA-PSO method was compared to six previously published works that aimed to minimize system power losses in microgrids. These works use either a single algorithm or a combination of hybrid or dual optimisation tools. The application of the research varied across authors, with some writers localized experiments and others used IEEE test beds to validate their results, as shown in table 4.

Table 4 Comparison of proposed technique with previous work

Author /Year	**Technique Used**	**Objective Functions**	**Platform**	**% of Losses**
Abdul-et al. 2018 [53]	CMFA	COE GHG	MATLAB	47.37
Hakim et al. 2020 [27]	PSO	Losses V/Profile	KDS14	40.50
Saad et al. 2021 [55]	Firefly Al	COE Losses	Rabel Model	44.44
Krishna et al 2022 [56]	MVO	COE Losses	MATLAB	18.34
Rene et al. 2023 [57]	GA-PSO	VDI Losses	MATLAB	35.87
Nasir et al. 2024 [7]	SMA	Losses V/Profile	MATLAB	48.53
Proposed Method	SMA-PSO	Losses V/Profile	MATLAB	49.61

4.0 CONCLUSION

In conclusion, the dual optimisation of SMA-PSO technique places the microgrid in a stable state while integrating 3,500 kW at the optimal location of bus 6. This result was due to the excess power of 26% and a power loss reduction of 49.64% which is sufficient to handle abrupt or surges in real power consumption. The increased redundancy capacity resulting from the integration of 4000 kW DG does not justify its optimality due to the greater cost associated with integrating a larger PV plant and the apparent reduced system power losses observed comparatively. The introduction of power capacities of 2000 kW and 2500 kW led to a fully saturated network without any excess stabilisation power. This result puts the network in a more vulnerable position with a lower reliability index.

The proposed SMA-PSO approach further validates the efficacy of the technique compared to previously published research on either single or hybrid optimisation methods over the last five years. The future work within the scope of the study should include an upgrade to more complex microgrids with a higher number of buses and further duality of other optimization algorithms.

Acknowledgement

The authors wished to thank Universiti Teknologi Malaysia for providing the necessary research facilities.

Conflicts of Interest

The author(s) declare(s) that there is no conflict of interest regarding the publication of this paper

References

[1] Amigue, F.F., et al., 2021. Optimal integration of photovoltaic power into the electricity network using Slime mould algorithms: Application to the interconnected grid in North Cameroon. *Energy Reports*, 7: 6292-6307.

[2] Arasteh, A., P. Alemi, and M. Beiraghi, 2021. Optimal allocation of photovoltaic/wind energy system in distribution network using meta-heuristic algorithm. *Applied Soft Computing.* 109: 107594.

[3] Roy, J.N.J., et al., 2023. Experimental investigation strategies to augment the diesel engine performance and reduction of emission characteristics by the effect of waste plastic oil. *ASEAN Engineering Journal,* 13(3): 47-53.

[4] Ansori, A., Et Al., 2023. Techno-Economic Analysis Of Triangular Rooftop Solar Pv Model/Pln On-Grid Household Scale In Indonesia. *ASEAN Engineering Journal,* 13(4): 127-132.

[5] Suberu, M.Y., et al., 2013. Power sector renewable energy integration for expanding access to electricity in sub-Saharan Africa. *Renewable and Sustainable Energy Reviews*, 25: 630-642.

[6] Yassim, H.M., et al., 2024. A review of hierarchical energy management system in networked microgrids for optimal inter-microgrid power exchange. *Electric Power Systems Research,* 231: 110329.

[7] Nasir, S.N.S., M.T. Ali, and J.J. Jamian. Determination of Optimal Power Flow for Photovoltaic Integration into Microgrid to Minimize System Losses Using Slime Mould Algorithm. in 2024 *IEEE 4th International Conference in Power Engineering Applications (ICPEA).* 2024. IEEE.

[8] Modu, B., et al., 2023. Energy management and capacity planning of photovoltaic-wind-biomass energy system considering hydrogen-battery storage. *Journal of Energy Storage*, 73: 109294.

[9] Houssein, E.H., et al., 2022. An efficient slime mould algorithm for solving multi-objective optimization problems. *Expert Systems with Applications*, 187: 115870.

[10] Olalo, J., C.J.D. Cruz, and K. Generoso, 2022. An Energy System Evaluation of Rural Electrification of Barangay Puray, Rodriguez, Rizal, Philippines. *ASEAN Engineering Journal*, 12(2): 151-159.

[11] Suchetha, C. and J. Ramprabhakar. 2019. Optimal power flow controller for a hybrid renewable energy system using particle swarm optimization. in *2019 National Power Electronics Conference (NPEC).* IEEE.

[12] Sulaima, M.F., et al., 2022. Determination Of The Optimum Load Profile Under Enhanced Of Use Tariff (Etou) Scheme Using Combination Of Optimization Algorithms And Self Organizing Mapping. *ASEAN Engineering Journal*, 12(4): 65-73.

[13] Avchat, H.S. and S. Mhetre. 2020. Optimal placement of distributed generation in distribution network using particle swarm optimization. in *2020 International Conference for Emerging Technology (INCET).* IEEE.

[14] D. K. Dhaked, S. Dadhich, and D. Birla, 2023. "Power output forecasting of solar photovoltaic plant using LSTM," *Green Energy and Intelligent Transportation*. 2(5): 100113

[15] Kouadri, R., et al., 2020. Optimal power flow control variables using slime mould algorithm for generator fuel cost and loss minimization with voltage profile enhancement solution. *International Journal of Emerging Trends in Engineering Research*. 8(1.1): 36-42.

[16] Naderipour, A., et al., 2021. Comparative evaluation of hybrid photovoltaic, wind, tidal and fuel cell clean system design for different regions with remote application considering cost. *Journal of Cleaner Production,* 283: 124207.

[17] Cortez, H.L., J.C.P. Broma, and G.V. Magwili. 2022. Optimal placement and sizing of hybrid solar-wind distributed generation in distribution network using particle swarm optimization algorithm. in 2022 *International Conference on Electrical, Computer and Energy Technologies (ICECET).* IEEE.

[18] Ali, B., et al., 2022 Power loss reduction of distribution network in densely industrialized coastal belt by development of hydrophobic coating applying accelerated aging for ceramic insulator. *ASEAN Engineering Journal*. 12(1): 111-117.

[19] Ghosh, S., S.P. Ghoshal, and S. Ghosh, 2010. Optimal sizing and placement of distributed generation in a network system. *International Journal of Electrical Power & Energy Systems,* 32(8): 849-856.

[20] Olalo, J., et al., 2022. Determination of a Potential for the Installation of Small-Scale Wind Turbine in Barangay Bagasbas, Daet Camarines Norte, Philippines. *ASEAN Engineering Journal,* 12(1): 17-26.

[21] Zahari, N.E.M., et al., 2024. Integrating Solar PV, Battery Storage, and Demand Response for Industrial Peak Shaving: A Systematic Review on Strategy, Challenges and Case Study in Malaysian Food Manufacturing. IEEE Access,

[22] Dharmavaram, A.D., 2024. Custom Ip Design And Verification For Ieee754 Single Precision Floating Point Arithmetic Unit. *ASEAN Engineering Journal.* 14(2): 69-76.

[23] Attia, A.-F., R.A. El Sehiemy, and H.M. Hasanien, 2018. Optimal power flow solution in power systems using a novel Sine-Cosine algorithm. *International Journal of Electrical Power & Energy Systems*. 99: 331-343.

[24] Tayab, U.B., et al., 2024. Optimum battery sizing, scheduling and demand management for microgrids using slime mould algorithm. *Journal of Energy Storage,* 91: 112034.

[25] Kanwar, N., et al., 2017. Simultaneous allocation of distributed energy resource using improved particle swarm optimization. *Applied energy,* 185: 1684-1693.

[26] Mostafa, M., et al., 2020. A new strategy based on slime mould algorithm to extract the optimal model parameters of solar PV panel. *Sustainable Energy Technologies and Assessments,* 42: 100849.

[27] Hassan, M.H., et al., 2021. Development and application of slime mould algorithm for optimal economic emission dispatch. *Expert Systems with Applications,* 182: 115205.

[28] Islam, M.Z., et al., 2020. A Harris Hawks optimization based single-and multi-objective optimal power flow considering environmental emission. *Sustainability,* 12(13): 5248.

[29] Widarsono, K., et al. 2020. Optimal power flow using particle swarm optimization for IEEE 30 bus. in *Journal of Physics: Conference Series.* IOP Publishing.

[30] Phyu, E.E., K.M. Lin, and T.T. Moe, 2018. Loss reduction and reliability improvement of industrial distribution system through network reconfiguration. *International Journal of Energy and Power Engineering,* 12(11): 807-813.

[31] Gao, Z., J. Zhao, and S. Li. 2020. The hybridized slime mould and particle swarm optimization algorithms. in *2020 IEEE 3rd international conference on automation, electronics and electrical engineering (AUTEEE*).. IEEE.

[32] Pan, J.-S., et al. 2018. S A novel hybrid GWO-FPA algorithm for optimization applications. in Advances in Smart Vehicular Technology, Transportation, Communication and Applications: Proceedings of the First *International Conference on Smart Vehicular Technology, Transportation, Communication and Applications, November 6-8,* 2017, Kaohsiung, Taiwan 1. pringer.

[33] Eappen, G. and T. Shankar, 2020. Hybrid PSO-GSA for energy efficient spectrum sensing in cognitive radio network. *Physical Communication,* 40: 101091.

[34] Şenel, F.A., et al., 2019. A novel hybrid PSO–GWO algorithm for optimization problems. Engineering with Computers, 35: 1359-1373.

[35] Suman, G.K., J.M. Guerrero, and O.P. Roy, 2021. Optimisation of solar/wind/bio-generator/diesel/battery based microgrids for rural areas: A PSO-GWO approach. *Sustainable Cities And Society*. 67: 102723.

[36] D. K. Dhaked, P. Kumar, and S. Ganguly, 2024 "Development of Data Driven Model for Proton Exchange Membrane Fuel Cell Using Machine Learning Approaches," in 2024 *IEEE 3rd International Conference on Control, Instrumentation, Energy & Communication (CIEC),* IEEE, 67-72.

[37] Abid, M.S., et al., 2023. Mitigating the effect of electric vehicle integration in distribution grid using slime mould algorithm. *Alexandria Engineering Journal*. 64: 785-800.

[38] Gómez, M., A. López, and F. Jurado, 2010. Optimal placement and sizing from standpoint of the investor of Photovoltaics Grid-Connected Systems using Binary Particle Swarm Optimization. *Applied Energy,* 87(6): 1911-1918.

[39] Li, S., et al., 2020. Slime mould algorithm: A new method for stochastic optimization. *Future generation computer systems,* 111: 300-323.

[40] Yassim, H.M., M.N. Abdullah, and C.K. Gan, 2024. A Comparison Of Power Flow Based On Bus Admittance Matrix For Networked Microgrid Energy Management Gy Management. *ASEAN Engineering Journal*,. 14(2): 27-35

[41] Charles, P., F. Mehazzem, and T. Soubdhan. Comparative study between Interior Point and Particle Swarm methods for Optimal Renewable Distributed Generation location. in *2020 6th International Conference on Electric Power and Energy Conversion Systems (EPECS)*. 2020. IEEE.

[42] Razzanelli, M., et al., 2020. Distributed model predictive control for energy management in a network of microgrids using the dual decomposition method. *Optimal Control Applications and Methods,* 41(1): 25-41.

[43] Castillo-Calzadilla, T., et al., 2022. Is a massive deployment of renewable-based low voltage direct current microgrids feasible? Converters, protections, controllers, and social approach. *Energy Reports*. 8: 12302-12326.

[44] Trivedi, R. and S. Khadem, 2022. Implementation of artificial intelligence techniques in microgrid control environment: Current progress and future scopes. *Energy and AI*. B: 100-147.

[45] Nasir, S.S., et al. 2022. Minimizing power loss in distribution system considering mass charging station operation. in *2022 IEEE International Conference on Power and Energy (PECon)*. IEEE.

[46] Malek, A.F., et al., 2023. Power distribution system outage management using improved resilience metrics for smart grid applications. *Energies,* 16(9): 3953.

[47] Bizimungu, S., et al., 2023. Analysis Of Rwanda's Grid Point Of Stability Loss. *ASEAN Engineering Journal,* 13(3): 1-14.

[48] Usama, M., et al., 2023. A multi-objective optimization of FCL and DOCR settings to mitigate distributed generations impacts on distribution networks. *International Journal of Electrical Power & Energy Systems,* 147: 108827.

[49] Shah, R., S. Jain, and K.C. Bandhu, 2024. Comparison And Evaluation Of Energy-Efficient Cloud Computing Techniques With Load Balancing Approaches. *ASEAN Engineering Journal.* 14(2): 121-133.

[50] Dung, H.T.K. and N.P. Khanh, 2022. Simulation Research on Interaction Between Wind and Solar Photovoltaics Systems. *ASEAN Engineering Journal*, 12(1): 141-148.

[51] Trivedi, G., et al. Optimal sizing and placement of multiple distributed generators using teaching learning-based optimization algorithm in radial distributed network. in *2019 6th International Conference on Control, Decision and Information Technologies (*CoDIT). 2019. IEEE.

[52] Alhadrawi, Z., M. Abdullah, and H. Mokhlis, 2022. A New Method To Enhance The Differential Protection Of The Microgrid By Self-Backup Protection. *ASEAN Engineering Journal*. 12(3): 19-25.

[53] Abdel-mawgoud, H., et al. 2018. Optimal installation of multiple DG using chaotic moth-flame algorithm and real power loss sensitivity factor in distribution system. in *2018 International Conference on Smart Energy Systems and Technologies (SEST).* IEEE.

[54] Hosseini, S.H.R., et al., 2020. Optimal planning and operation of multi-vector energy networks: A systematic review. *Renewable and Sustainable Energy Reviews*. 133: 110216.

[55] Saad, A.R., R.S. Wibowo, and D.C. Riawan. 2021. Minimizing the losses and cost of a radial network connected to DG, PV and batteries using firefly algorithm in Al-Bayda city, Libya. in *2021 International Conference on Artificial Intelligence and Mechatronics Systems (AIMS*). IEEE.

[56] Krishna, S., M. Deepak, and R. Sunitha. 2022. Optimal Scheduling of Distribution System with PV and Battery Energy Storage System. in *2022 IEEE Kansas Power and Energy Conference (KPEC). I*EEE.

[57] Rene, E.A., W.S.T. Fokui, and P.K.N. Kouonchie, 2023. Optimal allocation of plug-in electric vehicle charging stations in the distribution network with distributed generation. *Green Energy and Intelligent Transportation,* 2(3): 100094.